DESIGNING A CENTRIFUGAL FAN OF CARBON FIBER LAMINATE FOR HIGH CIRCUMFERENTIAL SPEED

Heiko RATTER[1], Hermann MAUCH[2], Benjamin HANGS[3],
Şaban ÇAĞLAR[1], Martin GABI[1]

[1] *Institude of Fluid MachineryKarlsruhe Institute of Technology, Kaiserstrasse 12, 76131 Karlsruhe, Germany*

[2] *Hürner-Funken GmbH, Nieder-Ohmener Straße, 35325 Mücke-Atzenhain, Germany*

[3] *Fraunhofer-Institute for Chemical Technology, Joseph-von-Fraunhofer-Str. 7, 76327 Pfinztal, Germany*

SUMMARY

Centrifugal fans made of plastic are commonly used in systems where the transported fluids containing acid materials. Nonmetallic materials have, additionally to their persistence against corrosion, the advantage of a low noise level. Conversely the low strength of plastic limits the load to the structure and hence the maximum circumferential velocity.
Within the scope of this project a given impeller design of plastic is optimized with the goal of higher efficiency and the ability of higher circumferential speed.
As material for the new fan carbon fiber laminate is chosen, due to its resistance against high stresses and persistence to acid materials. Because carbon fibers must be positioned without any sharp bends to avoid tension cracks, the use of such fiber materials restricts the design options of the fan. These requirements lead to a non-standard geometry especially at the intersections blade to shroud and blade to hub.
This paper presents the approach of designing an impeller geometry which fulfills all required restrictions. With the goal to construct a high efficient fan, 3D steady and unsteady CFD calculations of the impeller and the complete fan are carried out. They are based on a block structured mesh of 1.3 million cells for the impeller and inlet nozzle resp. 2.8 million cells for the complete fan.
21 different fan geometries were calculated, successively optimizing the impeller geometry. The calculations of the final impeller show higher efficiency rates at all given operation points, additionally the geometry fulfills all restrictions given by the material.

INTRODUCTION

Transported fluids containing acid materials cause destruction of steel and aluminum impellers, therefore centrifugal fans made of plastic are commonly used in these systems. Additionally to their persistence against corrosion, nonmetallic materials have the advantage of a low noise level. The low strength of plastic however limits the load to the structure and hence the maximum circumferential velocity. By gaining higher rotation speed, non-metallic fans can replace metallic ones, with all its advantages.

Within the scope of this project a given impeller design of plastic is optimized with the goal of higher efficiency and the tolerance to higher circumferential speed. Due to the carbon fiber laminate the geometry has to fulfill special restrictions. After a short overview of the material properties and restrictions, this paper describes the approach of designing a suitable fan geometry by conventional design methods and Computational Fluid Dynamic (CFD) calculations. The calculations are validated by measurements of the original geometry.

With the goal of not modifying the spiral casing, the main dimensions of the impeller are not changed.

FAN GEOMETRY

A CAD model of the basic impeller (g01) is shown in Fig. 1.The impeller consists of hub and shroud symmetric in rotational direction and 12 flat blades. Table 1shows the main dimensionless numbers of the impeller.

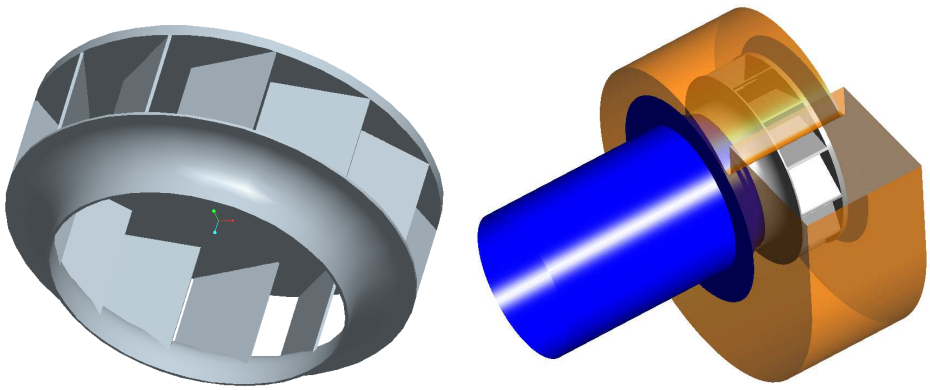

Fig. 1CAD model of the basic impeller and the complete fan (g01)

Table 1: Main dimensionless numbers of the basic fan geometry (g01)

Dimensionless number of:			
diameter - δ [-]	2.39	revolutions - σ [-]	0.44
volume flow - φ [-]	0.164	pressure - ψ_{fs} [-]	0.82

The kinetic energy at the exit of the spiral casing cannot be used and is therefore treated as loss; hence the efficiency of radial fans is calculated as follows:

$$\eta_{fs} = \frac{q_V p_{fs}}{P_S} = \frac{\varphi \psi_{fs}}{\lambda} \quad (1) \text{with } p_{fs} = p_{s2} - p_{t1} \quad (2)$$

The dimensionless numbers are given in (3)-(6). They are functions of the volume flow q_V, the pressure difference p_{fs}, the density of the fluid ρ, the outer impeller diameter D_2 and the circumferential velocity $u=2\pi D_2$.

$$\varphi = \frac{4q_V}{u\pi D_2^2} \quad (3) \qquad \psi_{fs} = \frac{p_{fs}}{\rho/2\, u_2^2} \quad (4) \qquad \delta = \frac{\psi^{0.25}}{\varphi^{0.5}} \quad (5) \qquad \sigma = \frac{\varphi^{0.5}}{\psi^{0.75}} \quad (6)$$

The dimensionless number of diameter and revolution shows, that the fan is located within the range where the highest efficiency rates are reached by diagonal fans [1]. Therefore the meridional shape of the impeller was slightly redesigned to obtain diagonal outflow conditions.

FIBER LAMINATE MATERIAL

Due to high loads caused by increased circumferential speed thermoplastic solutions with standard long- or short-fiber-reinforcement are not sufficient to fulfill the requirements of modern high-performance centrifugal fans. This is especially true with regard to the existent risk of creep under dynamic long term loads and in environments where aggressive chemicals are present. In consequence, the presented approach is based on novel continuously fiber-reinforced materials offering greatly improved mechanical properties compared to long- and short-fiber-reinforced alternatives. In particular unidirectionally carbon-fiber-reinforced polyphenylene sulfide (CF/PPS) tape is used. CF/PPS exhibits a superior strength-to-weight ratio combined with excellent chemical resistance, flame retardancy and long-term heat stability. Material specifications are listed in Table 2.

Table 2: Material properties of CF/PPS tape with an orientation of 0°

Density [g/cm³]	Fiber volume content [%]	Tensile strength [MPa]	Tensile modulus [GPa]	Elongation at break [%]	Flexural strength [MPa]	Flexural modulus [GPa]	Melt temp. [°C]
1.58	53	1.815	120.6	1.68	1.290	103.4	282

Nevertheless the use of material class restricts the design options of the fan. One constraint is that the fibers must be positioned without any sharp bends to avoid cracks in the carbon fibers and to optimize load paths in the fan. These requirements lead to a non-standard geometry, especially at the intersections blade to shroud and blade to hub.

The impeller is constructed by different parts - the hub, the shroud and one part for each blade. Each element is constructed by an individual way of the fibers. The last manufacturing process concatenates the three parts. Especially for the fibers of the blade, specific requirements are necessary.

Fig. 2 shows 4 different sketches of the intersection between blade and shroud. For simplification hub, shroud and blade are sketched as a line, and view is from a radial position outside the impeller.In Fig. 2 (a) the basic geometry is shown. The angle between the blade and hub (shroud) is named $\alpha_{BH}(\alpha_{BS})$.At the basic geometry both angles are rectangular $\alpha_{BH} = \alpha_{BS} = 90°$. Due to the fibers this form cannot be maintained.

The new geometry should have a smooth gradient at both intersections of blade to shroud and blade to hub.

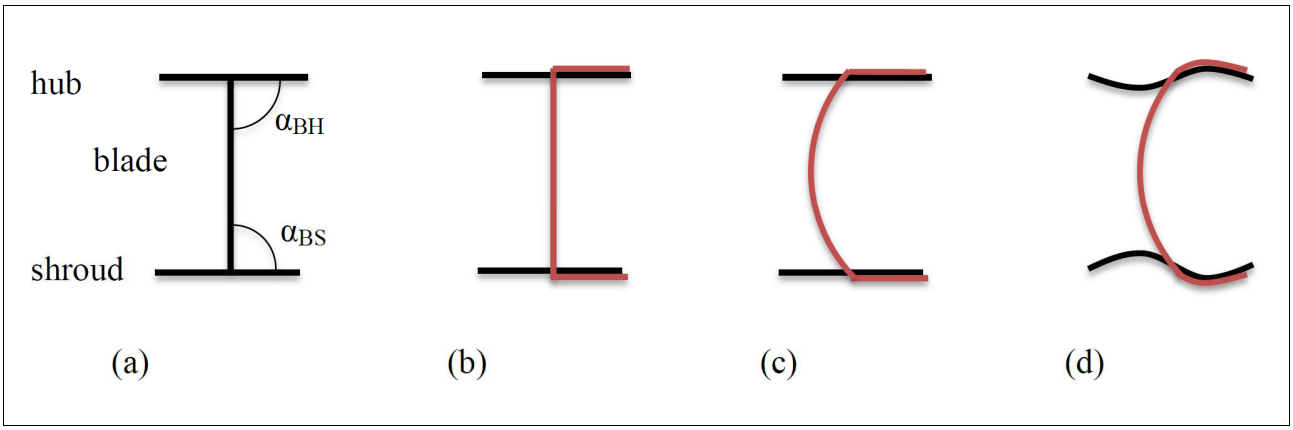

Fig. 2: Intersection between blade and shroud

The red line in Fig. 2(b) represents the fibers of the blade. Outside the hub and shroud they are bended over and pressed together, so that a compound is established. At the intersection position the shroud and hub therefore have to be cut. Fig. 2 (b) shows that by containing the basic geometry, the fibers will be bended by $\alpha_{BH} = \alpha_{BS} = 90°$ which might destroy them at load condition. To enlarge both angles, the blade can be designed as shown in Fig. 2(c). Furthermore to get an even higher angle the hub and shroud contour can be changed as demonstrated in Fig. 2(d). This leads to a nonsymmetrical shroud and hub in circumferential direction.

Due to the restriction of constant impeller main dimensions in this project the hub cannot be constructed in this nonsymmetrical "waveform". Otherwise the distance between the hub and the casing will be too small.

Fig. 3 shows the CAD model of the new impeller. Fig. 3 (a) shows the model which is calculated by CFD. Additionally the position of the blade fibers are shown in Fig. 3 (b) by the red structure. The lower part of the figure shows in detail the course of the blade fibers and the smooth intersection at the shroud.

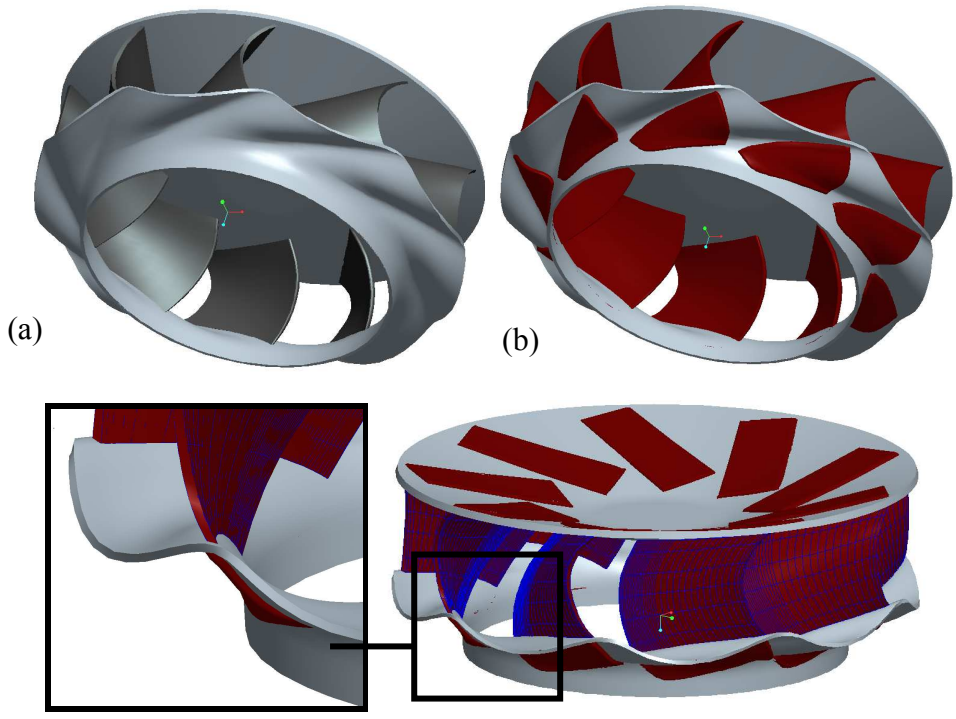

Fig. 3 CAD model of the optimized impeller (g21)

LAYOUT PROCESS

Fig. 4 shows the measured characteristic aerodynamic curve of the basic fan (g01). The goal of the new fan is, beside the mechanical restrictions, to get higher efficiency rates η_{fs} at the same operation points (φ,ψ_{fs}).

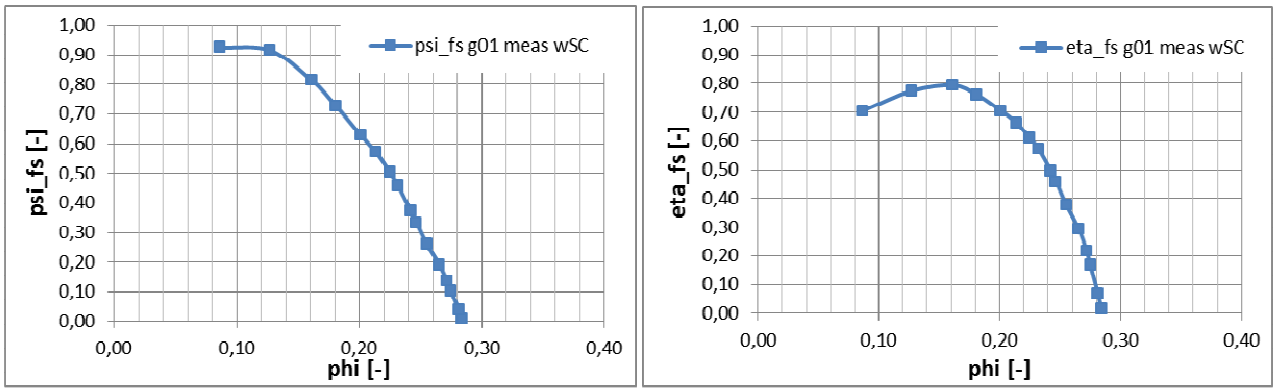

Fig. 4 Characteristic aerodynamic curve of (g01)

The knowledge of classical design processes implemented in computer algorithms allows designing an efficient fan for a certain operation point within a short time. To achieve very high efficiency rates, an iterative optimization process, with a lot of individual geometry changes, is necessary. Constructing and measuring these fans is cost-intensive and time consuming whereas numerical calculations are less expensive and faster.

In this project the first step of designing the impeller was done by using conventional layout algorithms. They were adapted with respect to the changing cross-section area due to the shroud.
The blade is constructed by 5 profile sections, each profile chord is constructed by a circular arc which is defined by the blade angles at the leading and trailing edge (β_{S1}, β_{S2}) and its diameters (D_{S1}, D_{S2}). The blade profile has a constant thickness with a rounded leading edge.

To achieve very high efficiency rates without manufacturing a lot of different geometries, CFD calculations were carried out.

CFD CALCULATIONS

CFD calculations at different operation points are performed, analyzed and taken as guidance for improving the fan. Solved are the RANS equations using the software package of ANSYS®-CFX. Fluid is treated as isotherm and incompressible. Turbulence is modeled by the *k*-ω-SST model with curvature correction[2]. The SST model has proven its reliability especially very well for adverse pressure gradient aerodynamic flows [3].

CFD Calculations of the complete fan

In a first step the complete fan including inlet nozzle, impeller and spiral casing was discretized by a 3D-blockstructured grid. Using a wall-function model for boundary layer treatment, the mesh was refined at the wall to reach a dimensionless wall distance y+ between 30 and 80. Avoiding strong changes in cell-ratios the mesh of the complete fan will consist of 12 million cells. A time resolved calculation with this amount of cells will take a lot of CPU time.It is considered, that for this optimization process, with calculations at different operation points the required calculation time with such a fine grid will be too high. Therefore a coarser grid of 2.8 million cells of the complete fan is used for unsteady calculations.

Fig. 5 shows the position of the boundary conditions (BC) for the calculations of the complete fan. Inlet-BC is set to total pressure p_t, outlet-BC to opening pressure p_s. Interface between rotating and stationary domain is done by a transient-rotor-stator interface.

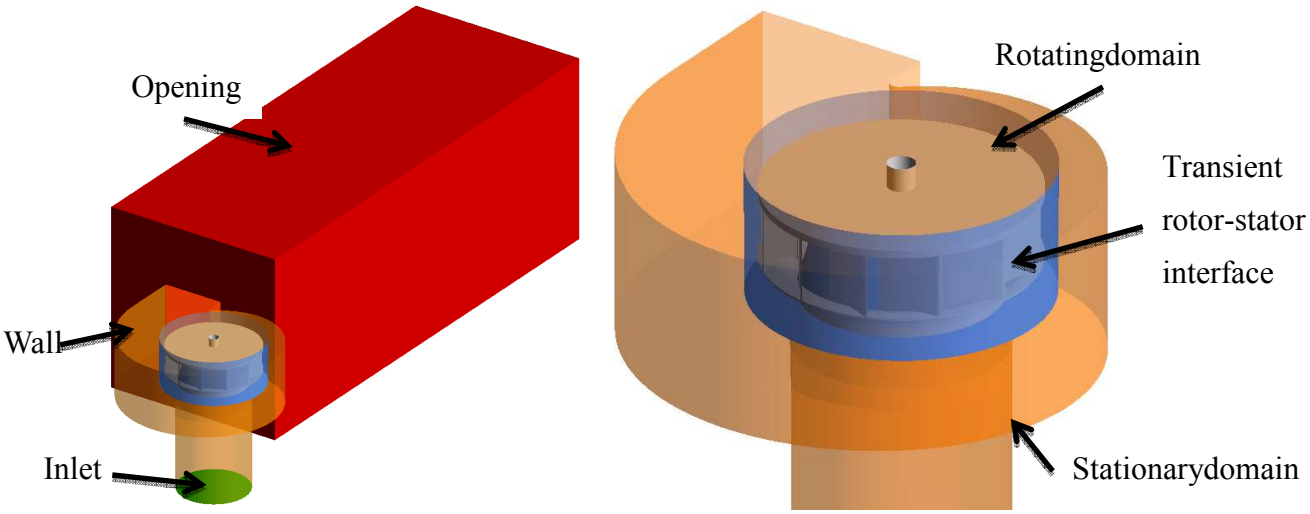

Fig. 5 Boundary Conditions for calculations of the complete fan

The convergence criterion is RMS≤10^{-4} for the inner iterations. The calculations were stopped when a stable periodic state and/or a constant mean value for the main values (q_V, η_{fs}) was reached. For one operation point the calculations took between 49-90 hours on 10 CPUs. Fig.6shows the calculated operation points in reference to the measured characteristic curve.

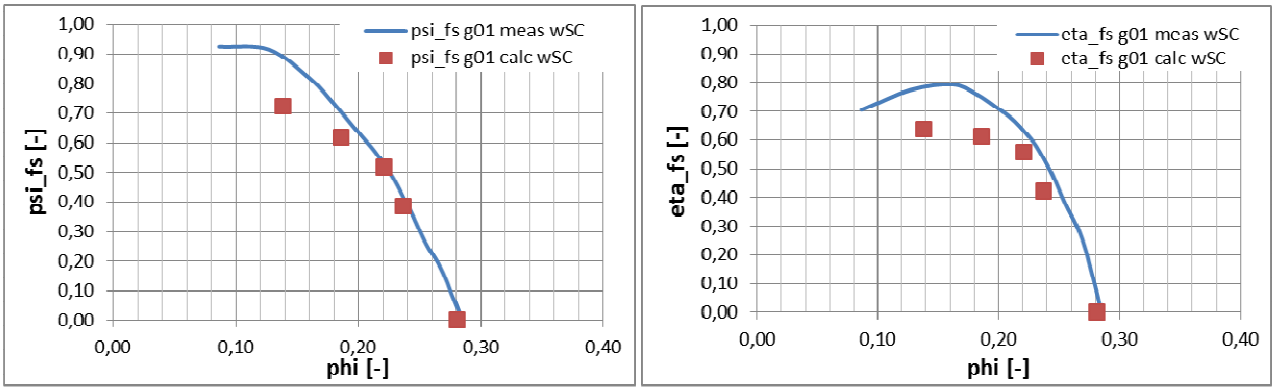

Fig.6 Measured curve vs. calculated points ofthe complete fan (g01)

There are small differences between measurement and calculation at high volume flow rates for pressure rise and efficiency.However the differences atbest point and partial load aretoo high for an optimization process. The authors see the reason for these differences in the very coarse grid.

CFD Calculations of impeller and nozzle without spiral casing

By disregarding the spiral casing, the mesh of the runner can be refined and calculation time can be reduced because of two reasons. Due to the periodicity in circumferential direction only one blade channel with periodic boundary conditions has to be calculated. Because there is additionally no time dependent interaction between the spiral casing and the impeller, the stationary RANS equations can be solved.

The total number of cells has been reduced to 1.3 million. However the number of cells per blade channel increased. As a result, the mesh is much smoother within the blade channel.

The impeller was optimized within 20 individual geometries. To present the results in a clear way only the last and best geometry (g21) is discussed.

Calculations are done on a PCin parallel mode by 6 Intel® Core™ i7 3.07 GHZ CPUs. The calculation of one operation point lasts between 2-4 hours.

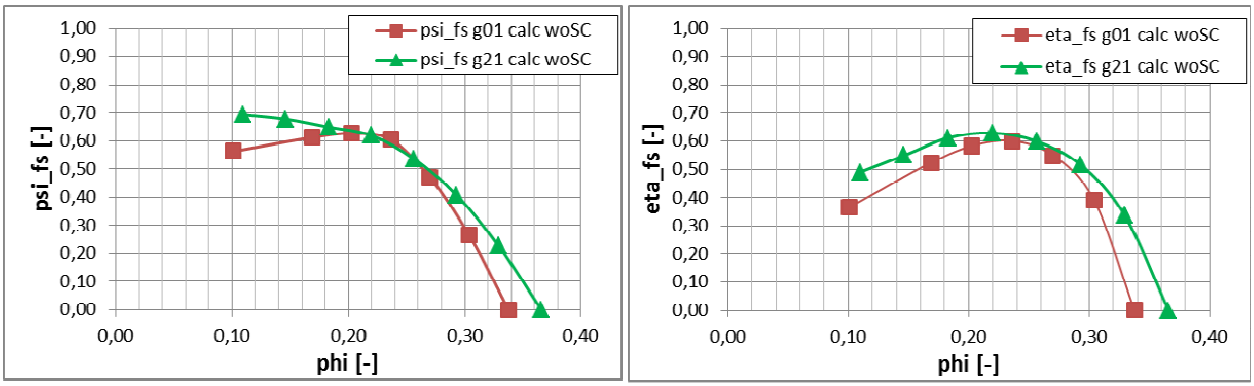

Fig. 7 Calculated characteristic curve of (g01) and (g21) without spiral casing

Fig. 7 shows the calculated performance of the basic (g01) and new (g21) geometry. At every volume flow rate the pressure difference of the basic impeller is reached by the new geometry and additionally the efficiency is higher.

Fig. 8 shows an isosurface of the relative velocity (blue) at the point of best efficiency. The value of the velocity is chosen small, so that most of the isosurface is located within the boundary layer. In areas where the contour of the isosurface does not look like the impeller geometry, separations occur (white arrows). The impeller g01 shows big areas of separations at the suction side of the blade especially close to the hub. The new impeller g21 also shows a separation at the exit of the blade, but much smaller compared tog01.

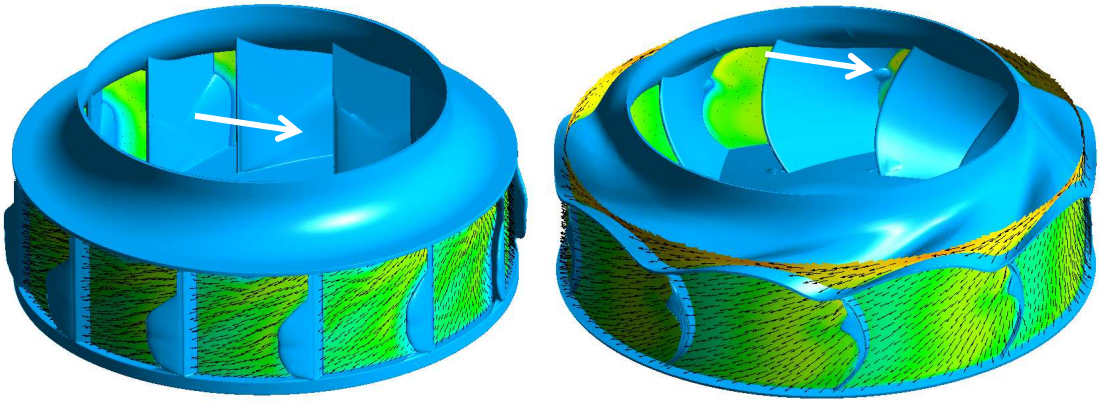

(g01) (g21)

Fig. 8 Isosurface of relative velocity (blue) and rotational surface with plotted relative velocity

CONCLUSION AND OUTLOOK

The new impeller was modeled in CAD, so that all required restrictions due to the used materials were fulfilled. CFD calculations show higher efficiency rates at all given operation points. Additionally the graphical analyzes shows a flow through the blade channels with only very small separations.

The optimized fan will be constructed by rapid prototyping methods for the validation of the CFD-calculations. If the efficiency rates at the operation points are reached, the fan will be constructed by fiber laminates and tested to its robustness.

ACKNOWLEGMENT

This work was supported by "ZentralesInnovationsprogrammMittelstand" (ZIM) of the Federal Ministry of Economics and Technology of Germany.

REFERENCES

[1] Cordier, O. – *Ähnlichkeitsbedingungen für Strömungsmaschinen* BWK, 337, **1953**

[2] Menter, F.-R. – *Zonal two equations k–ω turbulence models for aerodynamic flows*. AIAA paper 93-2906, **1993**

[3] Bardina, J. E.,Huang,T. J., and Coakley,T. J. – *Turbulence modeling, validation, testing and development*. NASA Technical Memorandum 110446, **1997**